# Trends in Applied Sciences Research

ISSN 1819-3579

Academic
Journals Inc.

www.academicjournals.com

Trends in Applied Sciences Research 7 (2): 132-141, 2012
ISSN 1819-3579 / DOI: 10.3923/tasr.2012.132.141


# Numerical Simulation of Tumor Development Stages Using Artificial Neural Network

[1]Ali Ahmadian, [2]Mohamed Bin Suleiman and [2]Fudziah Ismail
[1]Department of Mathematics, Mashhad Branch, Islamic Azad University, Mashhad, Iran
[2]Department of Mathematics, Faculty of Science, Universiti Putra Malaysia, 43400UPM, Serdang, Selangor, Malaysia

*Corresponding Author: Ali Ahmadian, Department of Mathematics, Mashhad Branch, Islamic Azad University, Mashhad, Iran*

## ABSTRACT

This study is developed a mathematical model to describe interactions between tumor cells and a compliant blood vessel that supplies oxygen to the region. In addition to proliferating, it is assumed that the tumor cells die through apoptosis and necrosis. It is also assumed that pressure differences within the tumor mass, caused by spatial variations in proliferation and degradation, cause cell motion. The behavior of the blood vessel is coupled into the model for the oxygen tension. The model equations tracked the evolution of the densities of live and dead cells, the oxygen tension within the tumor, the live and dead cell speeds, the pressure and the width of the blood vessel. This study presented the exact solutions to the model for certain parameter regimes and then solve the model with artificial neural networks for more general parameter regimes. This study also showed the resulting steady-state and porous medium behavior varies as the time is changed.

**Key words:** Numerical methods, nonlinear diffusion equations, neural network method, tumor cells, ordinary differential equations

## INTRODUCTION

There is many interesting researches about cancer and Tumor which has been done till now (Looi *et al*., 2006; Kumar *et al*., 2006; El-Naggar *et al*., 2011). Tumor development occurs in two distinct stages. Initially, tumor cells in small avascular tumors' gain the oxygen and nutrients they need for survival and growth by diffusion from the existing vasculature in the normal tissue that surrounds the tumor. The amount of oxygen thus supplied is limited by the surface area of the growing tumor while the amount of oxygen required by the cells is proportional to their total volume. In consequence, the tumor reaches a diffusion-limited size, where the amount of oxygen and nutrients entering balances the amount consumed by the live tumors cells (that exist near the rim of the tumor). The size of such a tumor is limited to 1-2 mm (Holmgren *et al*., 1995). The cells near the centre of such tumors are subjected to hypoxic stress (that is, low oxygen tensions which gradually `suffocate' the cells). Exposure to this stress slows their rate of proliferation and stimulates them to express diffusible factors such as Vascular Endothelial Growth Factor (VEGF), Tumor Necrosis Factor (TNF-$\alpha$), Transforming Growth Factor (TGF-$\beta$) which travel outwards from the tumor, towards the surrounding vasculature (Yazdi *et al*., 2011). Once these factors reach the surrounding blood vessels, they stimulate endothelial cells lining the walls of the blood vessels to proliferate, migrate and differentiate to form new blood vessels which grow towards the tumor.

Formation of new blood vessels by this process is called tumor angiogenesis (Bicknell *et al*., 1997; Homaei-Shandiz *et al*., 2009). Once the vessels have reached the tumor and circulatory loops have formed, blood can flow through the vessels and supply the tumor cells with additional oxygen and nutrients. Vascular tumor growth then commences. During vascular tumor growth, previously dormant cells that are close to the neovas-culature are able to proliferate once again and the growth of the tumor as a whole can recommence. This may become life threatening for the host, since, both the tumor and any metastases (secondary tumors that form when tumor cells escape from the primary tumor into the general blood or lymph circulation and establish colonies in other tissues) may cause malfunction of vital organs (Folkman, 1950). The tumor structure is heterogeneous: tumor cells in close proximity to blood vessels proliferate rapidly in the presence of abundant oxygen and nutrients (Hahnfeldt *et al*., 1999; Sodde *et al*., 2011) and where the rate of proliferation outstrips the rate of new blood vessel formation, transient areas of hypoxia form. Vascular tumors consist of a mixture of cell types, including live and dead tumor cells, macrophages and endothelial cells lining the blood vessels, all embedded in an extracellular matrix. Cells attach themselves to the extracellular matrix by expressing proteins and other molecules on their surface which bind to complementary molecules in the matrix (Alberts *et al*., 1994). There have been numerous mathematical models of avascular tumor growth (Byrne and Chaplain, 1995) for example. Such models normally prescribe the oxygen tension at the proliferating rim and may involve `compartmentalizing' the tumor into proliferating, quiescent and necrotic regions. There have also been several studies of angiogenesis (Byrne and Chaplain, 1995). However, only a small amount of (mathematical) literature concerns the growth of vascular tumors. Macro scale models (Byrne and Chaplain, 1995; Hahnfeldt *et al*., 1999) have been generated to describe various tumor phenomena: generate a model that describes how fluid moves out through the tumor's periphery; (Folkman, 1950; Ali *et al*., 2011) allows cell motion by diffusion and by taxis up gradients of capillary vessels and they calculate the density of live tumor cells and the surface area of the capillary vessels per unit volume. In this study, we present a mathematical model to describe the behavior of tumor development stages in time by use of porous medium equations and solve these by means of artificial neural network which help us to detect the time of beginning of each stage. The main differences between our model and numerical method with other are: fast convergence-the final solution is a function which we can use it to calculate other values of function at every point in training interval-some small errors, we can also change the neural network model or use heuristic optimization algorithms.

## MATHEMATICAL MODEL

We assume that the microenvironment within a tumor consists of a mixture of live and dead tumor cells, macrophages, extracellular water and endothelial cells (forming the tumor vasculature) embedded in a tissue matrix. The live tumor cells proliferate if the local oxygen tension is high enough and the rate at which proliferation occurs is assumed to be proportional to both the local oxygen tension and the (number) density of live cells. We assume that live cells can die by two processes. The first, apoptosis (Alberts *et al*., 1994) is programmed cell death (`old age') and occurs at all oxygen tensions. The rate of apoptosis may increase with decreasing oxygen tension (Hahnfeldt *et al*., 1999) but in this model we assume it is proportional to the local density of live cells and independent of the local oxygen tension The second death mechanism we consider is oxygen-induced-necrosis (henceforth termed necrosis) which we assume here to be cell death induced by oxygen starvation (suffocation). The rate of such necrosis is assumed to be proportional

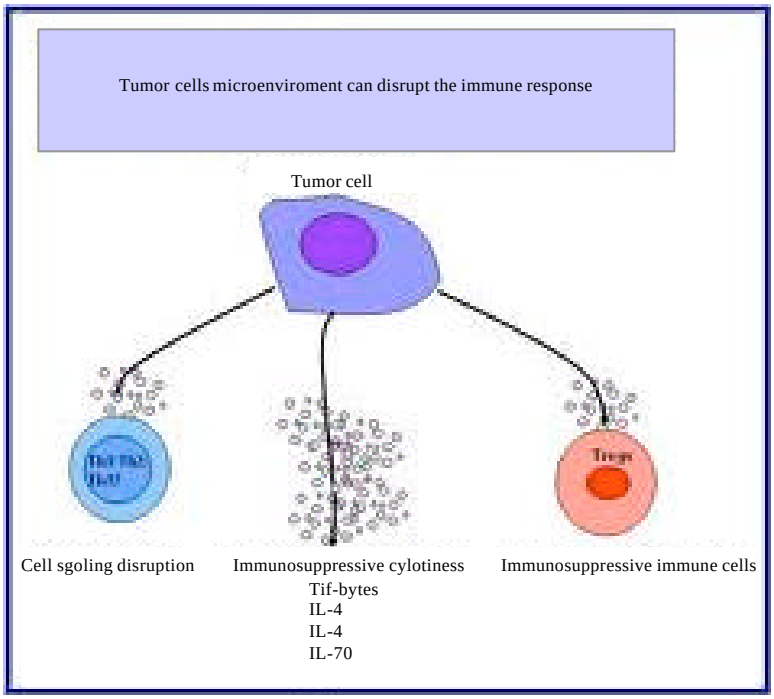


Fig. 1: Disrupting the immune response by tumor cells

to the local density of live cells and to be induced only when the oxygen tension drops below a threshold value. Other forms of necrotic cell death occur at all oxygen tensions, for example, necrosis due to low pH (Bicknell *et al*., 1997), we stress that we do not consider such mechanisms in this study. When live cells die by apoptosis, they become inactive but retain their form until they are either degraded by enzymes in the matrix or phagocytosed by macrophages (a type of stromal cell that moves around the tumor and accumulates in hypoxic areas) (Alberts *et al*., 1994). We suppose that these processes (which together we call degradation) occur at a rate proportional to the local density of dead cells Fig. 1. Cell proliferation and degradation in local sites throughout the tumor mass cause pressure gradients to be established. These, in turn, cause the blood vessel to open close and drive the movement of the live and dead cells. In this way the supply oxygen tension may vary due to changes in the local densities of the two cell types. We denote the density of live tumor cells by n, the density of dead tumor cells by and the oxygen tension by C. We let the live cells move with velocity $v_n$ and the dead cells move with velocity $v_m$. Using conservation of mass, we formulate the following equation to describe the evolution of the densities of live and dead tumor cells:

$$\frac{\partial n}{\partial t}+\frac{\partial (v_n n)}{\partial y}=\underbrace{\lambda nCH(C-C_1)}_{\text{Proliferation}}-\underbrace{An}_{\text{Apoptosis}}-\underbrace{NnH(C_2-C)}_{\text{Necrosis}} \tag{1}$$

$$\frac{\partial m}{\partial t}+\frac{\partial (v_m m)}{\partial y}=\underbrace{An}_{\text{Apoptosis}}-\underbrace{NnH(C_2-C)}_{\text{Necrosis}}-\underbrace{F_m}_{\text{Degradation}} \tag{2}$$

which proliferation does not occur (H is the Heaviside function), A is the apoptosis rate, N is the necrosis rate, $C_2$ is a threshold oxygen tension below which necrosis occurs, F is the dead cell degradation rate, y denotes the distance `outwards' from the blood vessel and t denotes time. In Eq. 1 and 2, we have also assumed that a live cell and a dead cell have the same volume. We note that when $C>C_1$ cells undergo proliferation and apoptosis.

When $C_1>C>C_2$ cells undergo apoptosis only and when $C<C_2$ cells undergo apoptosis and necrosis. We remark further that, since, the proliferation rate depends on the local nutrient concentration and since, the local nutrient concentration depends on the density of live cells Eq. 4, (1) does not automatically produce exponential tumor growth. Since, the total cell density remains constant, we have a further equation relating n and m, namely:

$$n+m = M \tag{3}$$

where, M is the (constant) density of live and dead cells at an arbitrary point within the tumor mass. A conservation of mass equation could also be formulated for the evolution of the density of the Struma. Since, we assume that this density is constant throughout the tumor mass, the equation would tell us the speed with which this component moved. We use conservation of mass to generate the equation governing the evolution of the oxygen tension C in the tumor. We assume that changes in C are due to advection, diffusion and consumption and so the resulting equation reads:

$$\frac{\partial C}{\partial t}+\frac{\partial}{\partial y}(v_{av}C) = \underbrace{D\frac{\partial^2 C}{\partial y^2}}_{\text{Diffusion}} - \underbrace{E_1 nC}_{\substack{\text{Consumption by}\\ \text{live tumor cells}}} - \underbrace{E_2 C}_{\substack{\text{Consumption}\\ \text{by stroma}}} \tag{4}$$

In Eq. 4, D is the diffusivity, $E_1$ is the rate at which live tumor cells consume oxygen and $E_2$ is the rate at which stromal cells consume oxygen. We have assumed, for simplicity, that oxygen advects with the (linear) phase averaged velocity, $v_{av}$, where:

$$v_{av} = \frac{nv_n + mv_m}{n+m} \tag{5}$$

The precise form for the advection velocity is immaterial, since, as we will see later in this section, in situations of practical interest the nondimensionalised leading order version of Eq. 4 is dominated by diffusion. We impose the following initial and boundary conditions on the tumor tissue. The initial density of live cells (and hence the density of dead cells) is prescribed. We assume the average cell speed $v_{av}$ at the vessel wall y = h matches the wall speed and no flow of cells across the line of symmetry out at y = L. We also assume symmetry of the oxygen tension about the symmetry line. These conditions are equivalent to prescribing:

$$n = n_0 \qquad \text{at} \qquad t = 0 \tag{6}$$

$$m = M - n_0 \qquad \text{at} \qquad t = 0 \tag{7}$$

$$v_{av} = \frac{\partial h}{\partial t} \qquad \text{at} \qquad y = h \tag{8}$$

$$v_n = v_m = 0 \qquad \text{at} \qquad y = L \tag{9}$$

$$\frac{\partial C}{\partial y} = 0 \qquad \text{at} \qquad y = L \tag{10}$$

where, $n_0$ is the initial density of live cells. We are now in a position to nondimensionalise the model. Since, we are interested in interactions between tumor cells and the blood vessel, we scale time with the tumor cell proliferation timescale ($\lambda C_0$). We scale lengths with half the intravascular distance (i.e., with L), the live and dead cell densities with the initial total density of cells (M) and we scale the oxygen tension with the oxygen that would be supplied by a vessel of width:

$$(h_B).\left(C_0 = \frac{h_B}{\alpha}\right)$$

We eliminate $v_n$ and $v_m$ from Eq. 1, 2 and 4 and the resulting nondimensionalised system of equations and boundary conditions reads (dropping primes):

$$\frac{\partial n}{\partial t} - \delta\sigma^* \frac{\partial}{\partial y}\left(n\frac{\partial P}{\partial y}\right) = ncH(C - C_1^*) - A^* n - N^* nH(C_2^* - C) \tag{11}$$

$$\frac{\partial m}{\partial t} - \sigma^* \frac{\partial}{\partial y}\left(m\frac{\partial P}{\partial y}\right) = A^* n + N^* nH(C_2^* - C) - F^* m \tag{12}$$

$$n + m = 1 \tag{13}$$

$$Pe\left(\frac{\partial C}{\partial t} - \sigma^* \frac{\partial}{\partial y}\left((m + \delta n)C\frac{\partial P}{\partial y}\right)\right) = \frac{\partial^2 C}{\partial y^2} - E_1^* nC - E_2^* C \tag{14}$$

with:

$$n = n_0 \qquad \text{at} \quad t = 0 \tag{15}$$

$$P + C = 1 \qquad \text{at} \quad y = \varepsilon h \tag{16}$$

$$-\sigma^*(m + \delta n)\frac{\partial P}{\partial y} = \varepsilon\frac{\partial h}{\partial t} \qquad \text{at} \quad y = \varepsilon h \tag{17}$$

$$\frac{\partial P}{\partial y} = 0 \qquad \text{at} \qquad y = 1 \tag{18}$$

$$\frac{\partial C}{\partial y} = 0 \qquad \text{at} \qquad y = 1 \tag{19}$$

The non-dimensional parameter groups introduced into Eq. 11-19 are defined below as:

$$A^* = \frac{A}{\lambda C_0}, N^* = \frac{N}{\lambda C_0}, F^* = \frac{F}{\lambda C_0}, \varepsilon = \frac{h_B}{L}, C_1^* = \frac{C_1}{C_0}, C_2^* = \frac{C_2}{C_0}, Pe = \frac{\lambda C_0 L^2}{D}, E_1^* = \frac{E_1 M L^2}{D}, E_2^* = \frac{E_2 L^2}{D}, \delta = \frac{\sigma_1}{\sigma_2}, \sigma^* = \frac{\sigma_2 \alpha k}{\lambda L^2} \tag{20}$$

We now estimate that two of the parameters are small:

- $\varepsilon \sim 0.02 \ll 1$, for blood vessels of width $h_B = 10$ μm and a tumor intravascular distance of 1 mm (so that $L = 5 \times 10^{-4}$ m)
- $Pe \sim 0.03 \ll 1$, for diffusivity $D \sim 10^{-10}$ m$^2$ sec$^{-1}$ and with a proliferation timescale of 1 day ($\lambda C_0 \sim 10^5$ sec)

Thus, we take the limits $\varepsilon \to 0$, $Pe \to 0$, with consequences that the blood vessel boundary conditions are applied on $y = 0$, the speed of the cells at the blood vessel wall is zero and the problem for the oxygen tension becomes quasi-steady.

**Numerical solutions by means of artificial neural network:** Consider the equation Eq. 11 with assumed boundary conditions (Myers, 1996). The suggested trial solution can be as (Lagaris *et al*., 1998; Al-Daoud, 2009; Effati *et al*., 2010; Tortoe *et al*., 2011):

$$u_T(x,t,P) = \frac{(t-t_0)}{(t_1-t_0)} B(x) + \frac{(t-t_1)}{(t_0-t_1)} A(x) + (t-t_0)(t-t_1) N(x,t,P) \tag{21}$$

where, N is the neural network and P contains the weights of neural network model (Asadollahi-Baboli, 2011; Senol and Ozturan, 2008; Olanrewaju *et al*., 2011; Khalaf *et al*., 2011; Yu *et al*., 2011). The neural network architect is similar to Fig. 2:

Indeed the weight vector P contains the weights of input layer (W), bias vector (b) and the weights of output layer (V). "sigmoid" is the activation function of the network:

$$f_s(n) = \frac{1}{1+\exp(-n)}$$

Sigmoid transfer function is plotted in Fig. 3.

It is easy to check that the trial solution Eq. 21 satisfies the conditions Eq. 15-19. Suppose that $x \epsilon [x_0, x_1]$ and $t \epsilon [t_0, t_1]$. Now putting Eq. 21 in 11 we have:

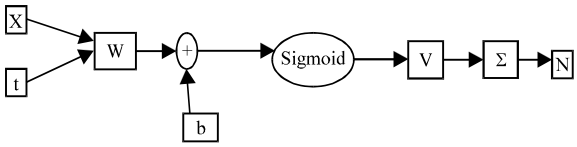


Fig. 2: Neural network architect

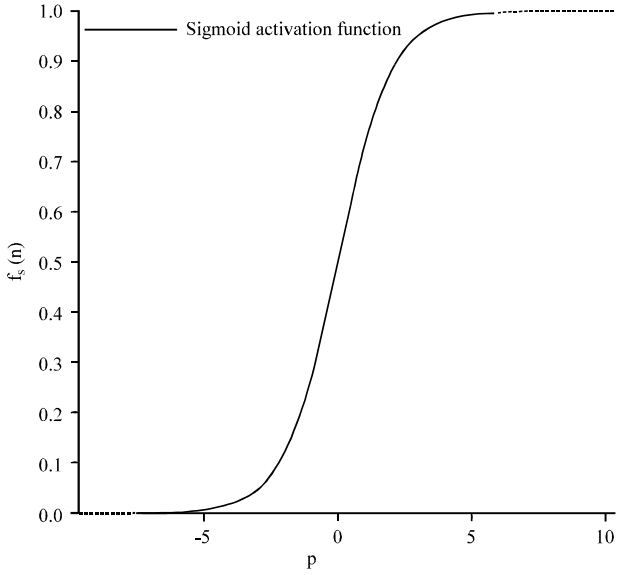


Fig. 3: Sigmoid activation function

$$\frac{\partial u_T(x,t,P)}{\partial t} = -\frac{\partial}{\partial x}(u_T(x,t,P)^n \frac{\partial^3 u_T(x,t,P)}{\partial x^3}) \tag{22}$$

We define the following optimization problem:

$$\underset{P}{Min} \sum_{i=1}^{n} \{\frac{\partial u_T(x_i,t_i,P)}{\partial t} + \frac{\partial}{\partial x}(u_T(x_i,t_i,P)^n \frac{\partial u^3{}_T(x_i,t_i,P)}{\partial x^3})\}^2 \tag{23}$$

Equivalently if we define:

$$\Psi(x,t,P) = \frac{\partial u_T}{\partial t} + \frac{\partial}{\partial x}(u_T^n \frac{\partial^3 u_T}{\partial x^3})$$

Then we have the following optimization problem:

$$\underset{P}{Min} \sum_{i=1}^{n} \{\Psi(x_i,t_i,P)\}^2 \tag{24}$$

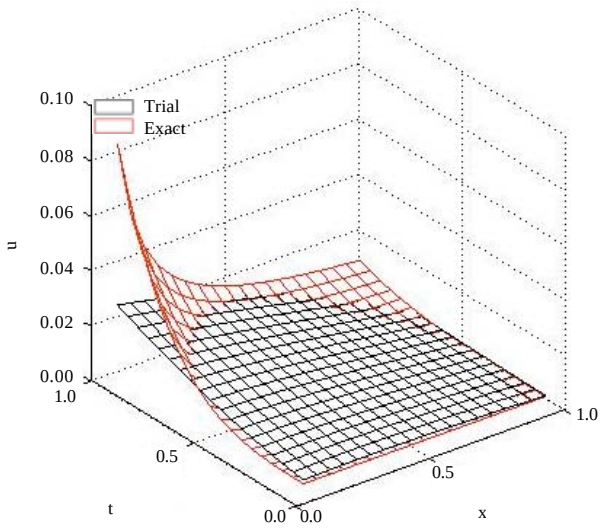


Fig. 4: Exact and approximated solutions of the development stages of tumor

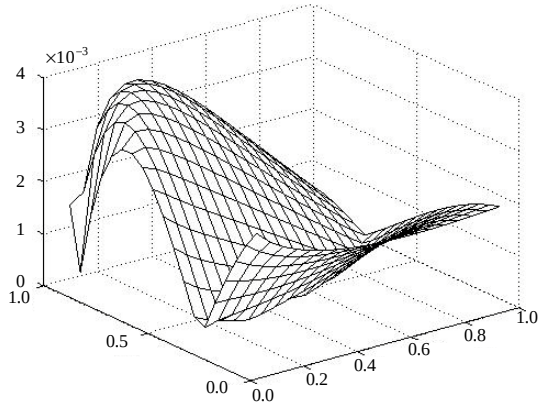


Fig. 5: Error $L^2$

To solve Eq. 24 we can use any optimization algorithms such as the steepest descent method and the conjugate gradient or quasi-Newton methods. The Newton method is one of the important algorithms in nonlinear optimization. The main disadvantage of the Newton method is that it is necessary to evaluate the second derivative matrix (Hessian matrix). In this paper we use quasi-Newton BFGS method, however, we can use heuristic algorithms such as PSO,GA and ACO. The most fundamental idea in quasi-Newton methods is the requirement to calculate an approximation of the Hessian matrix (Ahmadian and Afsharinafar, 2011). After the optimization step, we replace the optimal values of weight vector P in to the Eq. 21 which is the final solution. The exact and approximated solution can be found in Fig. 4 and 5. To solve this problem we used MATLAB 7 optimization toolbox using the BFGS hessian updater.

## CONCLUSION

We have presented a mathematical model to describe micro scale interactions between tumor cells and a compliant blood vessel within a vascular tumor. When developing he model, we assumed that the tumor mass comprised a mixture of live and dead cells. Analytical and numerical technique

were utilized to illustrate the qualitative behavior of the model solutions and the system was observed to settle to a steady state (Fig. 4).

## REFERENCES

Ahmadian, A. and R. Afsharinafar, 2011. An approximation method for solving nonconvex quadratic programming problems. J. Applied Sci., 11: 3807-3810.

Al-Daoud, E., 2009. A comparision between three neural network models for classification problems. Int. Artif. Intell., 2: 56-64.

Alberts, B., D. Bray, J. Lewis, M. Raff, K. Roberts and J.D. Watson, 1994. Molecular Biology of the Cell. 3rd Edn., Garland Publishing, New York, USA., ISBN-13: 978-0815316190, Pages: 1408.

Ali, R., A.M. Alabsi, A.M. Ali, Ainideris, A.R. Omar and K. Yousoff, 2011. Apoptosis induction and cytolytic effects of newcastle disease virus strain Af2240 on DBTRG.05 mg brain tumor cell line. Int. J. Cancer Res., 7: 25-35.

Anderson, A.R.A. and M.A.J. Chaplain, 1998. Continuous and discrete mathematical models of tumor-induced angiogenesis. Bull. Math. Biol., 60: 857-900.

Asadollahi-Baboli, M., 2011. Effect of weight updates functions in QSAR/QSPR Modeling using artificial neural networks. J. Artif. Intell., 4: 257-268.

Bicknell, R., C.E. Lewis and N. Ferrara, 1997. Tumor Angiogenesis. Oxford University Press, UK., Pages: 281.

Byrne, H.M. and M.A. Chaplain, 1995. Mathematical models for tumor angiogenesis: Numerical simulations and nonlinear wave solutions. Bull. Math. Biol., 57: 461-486.

Effati, S. and M. Pakdaman, 2010. Artificial neural network approach for solving fuzzy differential equations. Inform. Sci., 180: 1434-1457.

El-Naggar, S.A., A. El-Brabary, M.A. Mansour, F. Abdel-Shafy and S. Talat, 2011. Anti-tumor activity of some 1,3,4-thiadiazoles and 1,2,4-triazine derivatives against ehrlichs ascites carcinoma. Int. J. Cancer Res., 7: 278-288.

Folkman, J., 1950. Tumour angiogenesis. Adv. Cancer. Res., 43: 175-203.

Hahnfeldt, P., D. Panigrahy, J. Folkman and L. Hlatky, 1999. Tumor development under angiogenic signaling: A dynamic theory of tumor growth, treatment response and postvascular dormancy. Cancer Res., 59: 4770-4775.

Holmgren, L., M.S. O'Reilly and J. Folkman, 1995. Dormancy of micrometastases: Balanced proliferation and apoptosis in the presence of angiogenesisA suppression. Nature Med., 1: 149-153.

Homaei-Shandiz, F., G. Maddah, A. Aledavood, M.M. Marjaneh and K. Ghaffarzadehgan *et al.*, 2009. Pretreatment serum squamous cell carcinoma antigen levels in esophageal squamous cell carcinoma. Int. J. Cancer Res., 5: 53-57.

Khalaf, E.F., K. Daqrouq and M. Sherif, 2011. Wavelet packet and percent of energy distribution with neural networks based gender identification system. J. Applied Sci., 11: 2940-2946.

Kumar, R.V., V. Ravikumar, K.S. Shivashangari, S. Kamaraj and T. Devaki, 2006. Chemopreventive role of lycopene and d-arginine in benzo (a) Pyrene induced lung cancer with reference to lipid peroxidation, antioxidant system and tumor marker enzymes. Int. J. Cancer Res., 2: 224-233.

Lagaris, I.E., A. Likas and D.I. Fotiadis, 1998. Artificial neural network for solving ordinary and partial differential equations. IEEE Transact. Neural Networks, 9: 987-1000.

Looi, M.L., M.D.A.Z. Hatta, M.A.S. Aishah, M.H. Baizurah, W.N. Wan Zurinah and M.Y.Y. Anum, 2006. Serum levels of squamous cell carcinoma antigen and CA 125 in cervical intraepithelial neoplasia and invasive squamous cell carcinoma of the uterine cervix. Int. J. Cancer Res., 2: 212-218.

Myers, T.G., 1996. Surface Tension Driven Thin Film Flows. John Wiley and Sons, New York.

Olanrewaju R.F., O.O. Khalifa, A. Abdullah, A.A. Aburas and A.M. Zeki, 2011. Determining watermark embedding strength complex valued neural network. J. Applied Sci., 11: 2907-2915.

Senol, D. and M. Ozturan, 2008. Stock price direction prediction using artificial neural network approach: The case of Turkey. J. Artif. Intell., 1: 70-77.

Sodde, V., N. Dashora, K.S. Prabhu and R. Lobo, 2011. Evaluation of anticancer activity of *Macrosolen parasiticus* (L.) danser on ehrlich's ascites carcinoma treated mice. Int. J. Cancer Res., 7: 135-143.

Tortoe, C., J. Orchard, A. Beezer and J. Teetheh, 2011. Application of radial basis function network with a gaussian function of artificial neural networks in osmo-dehydration of plant materials. J. Artif. Intell., 4: 233-244.

Yazdi, H.S., M. Pakdaman and H. Modaghegh, 2011. Unsupervised kernel least mean square algorithm for solving ordinary differential equations. Neurocomp., 74: 2062-2071.

Yu, K.C., Y.H. Hung, S.H. Hsieh and S.J. Hung, 2011. Chiller energy saving optimization using artificial neural networks. J. Applied Sci., 11: 3008-3014.